International Journal of Thermophysics, Vol. 26, No. 1, January 2005 (© 2005)
DOI: 10.1007/s10765-005-2358-y

Subpicosecond Observation of Photoexcited Carrier Thermalization and Relaxation in InP-Based Films[1]

J. Michael Klopf[2] and Pamela M. Norris[3,4]

Advancements in microfabrication techniques and thin film growth have led to complex integrated photonic devices. The performance of these devices relies upon precise control of the band gap and absorption mechanisms in the thin film structures, as well as a fundamental understanding of the photoexcited carrier thermalization and relaxation processes. Using a pump-probe technique, it is possible to monitor the transient thermalization and relaxation of hot electrons and holes on a sub-picosecond time scale. This method relies upon the generation of hot carriers by the absorption of an intense ultrashort laser pulse (~135 fs). Transient changes in reflectance due to the pump pulse excitation are monitored using a weaker probe pulse. Control of the relative time delay between the pump and probe pulses allows for temporal measurements with resolution limited only by the pulse width. The transient change in reflectance is the result of the transient change in the electron and hole distributions. Observation of the reflectance response of InP films on a subpicosecond timescale allows for detailed examination of thermalization and relaxation processes of the excited carriers. Longer timescales (>100 ps) are useful for correlating the transient reflectance response to slower processes such as thermal conduction and recombination. A description of this technique and results for several InP-based films are presented.

KEY WORDS: InP; split-off band; subpicosecond; transient reflectance.

[1]Paper presented at the Fifteenth Symposium on Thermophysical Properties, June 22–27, 2003, Boulder, Colorado, U.S.A.

[2]Department of Engineering Physics, University of Virginia, Charlottesville, Virginia 22904, U.S.A.
[3]Department of Mechanical and Aerospace Engineering, University of Virginia, Charlottesville, Virginia 22904, U.S.A.
[4]To whom correspondence should be addressed. E-mail: pamela@virginia.edu

1. INTRODUCTION

The continuing development of solid-state photonic devices based upon various III–V semiconductors has created numerous advances in the technologies associated with communications, data storage, laser machining and cutting, and biomedical applications, as well as in many fields of basic science research. These small devices have very low power requirements, and can be integrated directly with power and control electronics, resulting in optoelectronics that are more efficient than multicomponent systems. The production of passive elements such as waveguides or active elements, such as amplifiers and switches, combine to expand the capabilities greatly. These devices rely upon layers of band-gap engineered materials with critical dimensions on the order of nanometers [1]. The resulting interfaces create localized changes in the band structure which can affect absorption and recombination processes [2,3]. Continued developments require ongoing research into the carrier dynamics in bulk materials as well as nanostructures.

Photonic semiconductor materials generally exhibit a direct band-gap electronic structure. The direct alignment of the conduction band minimum and valence band maximum makes radiative recombination of electrons and holes very likely, giving rise to many of the photonic properties of interest. The generation of excess conduction electrons is possible through the absorption of photons with energy, E_γ, greater than the band gap, E_g. Since recombination of these electrons occurs primarily near the conduction band minimum, an energy in excess of the band gap, $E_\Delta = E_\gamma - E_g$, must be transferred to the crystal through relaxation processes [4]. The absorption characteristics of the film are affected by both the number of photoexcited carriers, as well as the location of the occupied states in the conduction band. Similarly, the number and occupation of hole states generated by photon absorption will have an impact on the absorption of the film. Conduction electrons with $E_\Delta > 0$ (*hot electrons*), lose energy primarily through electron–phonon (e–p) collisions. The initial excitation and subsequent relaxation of the electron and hole distributions induce changes in the absorption spectrum [4]. Measurement of the changes in absorption during hot electron relaxation is an important goal of this study and should prove beneficial in the continuing development of photonic devices.

2. CARRIER THERMALIZATION AND RELAXATION PROCESSES

In direct band-gap semiconductors, photon absorption above the fundamental absorption edge occurs primarily through interband transitions,

resulting in electron-hole pair generation. Following this, the electron system is left in an excited state and will return to a lower energy state through various relaxation processes. The hole system follows a similar process, but the discussion here will be limited to the electron system. In this discussion it will also be necessary to consider absorption occurring on extremely short time scales. The experiments presented here use laser pulses ~135 fs in duration, but even shorter pulses are possible. Absorption on this time scale produces a coherent redistribution of the electron system representative of the participating transitions. In the case of excitation by monochromatic light, initially the hot electron distribution will be sharply peaked in the region of the direct transition for that energy. Through thermalization and relaxation processes, the hot electrons will scatter away from the initial excited distribution to the bottom of the conduction band before recombining [5].

These processes occur on time scales ranging from $\lesssim$ 200 fs to greater than 100 ps; thus, it is useful to consider several regimes of interest. Table I lists these and the respective relaxation and scattering processes occurring in each [4]. These regimes are useful for characterizing the hot carrier distribution. Initially in the *coherent regime*, it is possible to have a discontinuous hot carrier distribution. Thermalization of the hot carriers will occur during this period through scattering processes in order to reach

Table I. Transient Thermalization and Relaxation Regimes [4]

Time scales for thermalization and relaxation of hot carriers
Coherent Regime ($\leqslant$200 fs)
• momentum scattering
• carrier-carrier scattering
• hole-optical phonon scattering
Nonthermal Regime ($\leqslant$2 ps)
• electron-hole scattering
• electron-optical phonon scattering
Hot Excitation Regime ($\sim 1 \sim 100$ ps)
• carrier-acoustic phonon scattering
• decay of optical phonons
Isothermal Regime ($\geqslant$100 ps)
• carrier recombination
Time

a continuous, yet nonthermal distribution. In the following *nonthermal regime*, relaxation occurs as hot carriers drop towards the conduction band minimum, releasing energy through collisions primarily with optical phonons. Further relaxation occurs in the *hot excitation regime* through additional collisions with acoustic phonons. These leave the electrons near the conduction band minimum in the *isothermal regime* when recombination occurs.

The scattering rates of these processes vary depending on the carrier concentration as well as the average carrier energy and the film temperature. The density of photoexcited carriers will have a strong effect on electron–electron (e–e) scattering as well as a screening effect on the e–p scattering [4]. Experiments to observe e–e scattering in GaAs films have been pursued by other groups at low temperatures [5,6]. Under these conditions this process will dominate in samples of high purity, but at room temperature and low carrier densities, the e–e scattering rate (τ_{ee}^{-1}) is significantly less than the electron–phonon (e–p) scattering rate (τ_{ep}^{-1}) [7]. At sufficiently high carrier densities, e–e scattering may become important, and will be examined as part of this study.

3. EFFECT ON OPTICAL PROPERTIES

Considering an ultrashort laser pulse with photon energy, E_γ, greater than the band gap, E_g, absorption will occur primarily through interband transitions resulting in the generation of hot electrons. In general, this results in a reduction in the number of states available for interband photon absorption. Initially, absorption near the excitation energy is suppressed due to the coherent redistribution of electrons into states participating in transitions at E_γ. As the hot electrons thermalize and relax, the absorption at this energy will increase. Transient changes in the hot carrier distribution due to the various scattering processes cause transient changes in the absorption characteristics of the film.

In many studies of hot carrier dynamics, the absorption characteristics are determined through transmission measurements made on either free standing films, or films bonded to a substrate transparent throughout the spectral range of interest. With this technique, sample preparation can prove difficult and can often render the films unusable in a device application. In the study presented here, measurements of the transient change in reflectance, $\Delta R/R$, were made on nontransmissive films. Because of this, no further sample preparation is required following film growth. Changes in the $\Delta R/R$ signal should be indicative of changes in the transient absorption of the film.

It is important to note that significant changes in the reflectance can occur as the photon energy is increased above the threshold for certain transitions. Examination of the band structure of InP reveals transitions from the spin–orbit split-off (s–o) band to the conduction band for $E_\gamma > E_\gamma + \Delta$, where Δ is the s–o band offset, in addition to the direct transitions originating from the top of the heavy and light hole valence bands. Transitions from the s–o band are allowed through only part of the tuning range of the laser, whereas transitions from the heavy and light hole bands occur throughout. In doped crystals, the donor and acceptor states can also participate in the absorption processes [8] as well as cause band narrowing at high concentrations [9,10]. These transitions must be taken into account when necessary.

Carrier concentration-dependent effects can become significant for high intensity photoexcitation and are examined in this study as well. Both theoretical as well as experimental results have been reported on effects such as the concentration dependence of the effective mass [10], band-gap narrowing [11], and the shift in the absorption edge described by Burnstein and Moss [12,13]. The Burstein–Moss effect is due to the filling of states at the bottom of the conduction band, resulting in a shift of the absorption edge to a higher energy. This requires relaxation of the hot carriers to occur before becoming significant. The other effects, however, rely upon Coulomb screening and electron exchange interactions [10] which alter absorption through changes induced in the density of states, $D(\varepsilon)$. Bleaching is similar to the Burstein–Moss effect since it occurs as a result of the filling of states around a given optical transition. When the filling of states reaches saturation, absorption is suppressed at the given photon energy, resulting in a bleaching of that optical transition [14]. Investigation of evidence of concentration-dependent effects on the $\Delta R/R$ signal is presented here as well.

4. EXPERIMENTAL SETUP

The experimental setup used for this study is based upon a typical pump-probe configuration and is depicted in Fig. 1. This technique has been employed by many to resolve fast transient processes with picosecond resolution as early as 1974 [15]. Later, groups such as Paddock and Eesley applied this method to perform thermal diffusivity measurements in thin metallic films [16]. In the experiment presented here, a passively mode-locked Ti:sapphire laser is used to produce the ultrashort pulses ($\tau_p \sim 135$ fs) required for this study. The pulses are generated at a repetition rate of 76 MHz and are tunable over a wavelength range of 720–860 nm. The beam is split and follows two paths, the pump and the probe path.

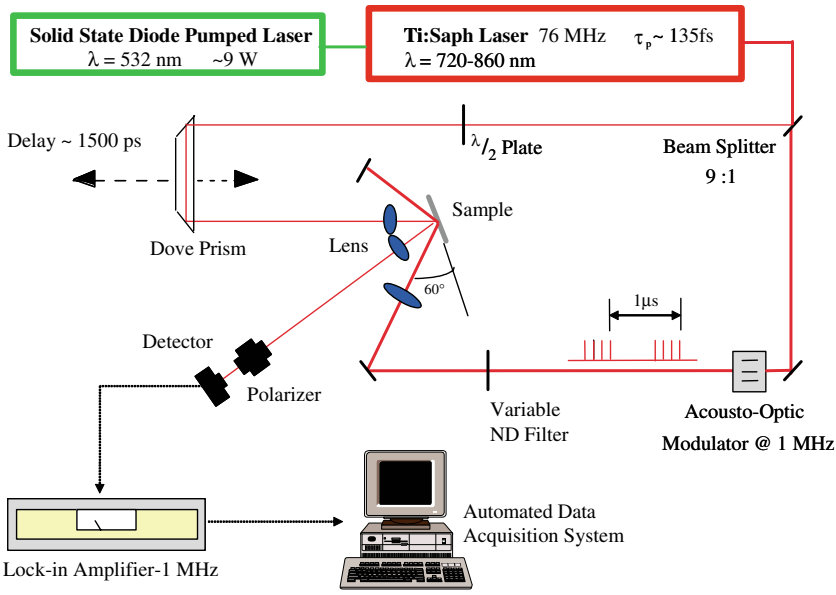

Fig. 1. Experimental setup for spectrally resolved transient reflectance measurements.

In the probe beam path, a half-wave plate rotates the polarization by 90° to allow scattered pump light to be eliminated by a polarizer before detection. The pump and probe beams are focused onto the sample with diameters of ~35 and ~ 5μm, respectively. The probe is focused at the center of the pump beam on the sample, ensuring isometric excitation in the plane of the film at the probe beam focus. The pump path length is fixed while the probe path length can be varied using a linear micropositioning stage. This allows for control of the probe path length in less than 10 fs increments such that the probe pulse arrives before, during, or after the pump pulse. The pump beam is modulated by an acousto-optic modulator (AOM) at 1 MHz resulting in a modulated excitation of the sample. The modulated carrier excitation produced by the pump beam results in a modulation of the optical properties observed as a change in the reflectance. This small change in reflectance is measured by a lock-in amplifier referenced to the 1 MHz modulation frequency. The initial excitation and subsequent relaxation of the hot carrier distribution are detected through transient reflectance data [4, 17].

The reflected probe pulses are focused onto a high speed Si PIN photodetector. The output of this detector is measured by the lock-in amplifier. As the probe path is varied in discrete steps, transient reflectance

data are taken by recording the magnitude and phase of the change in the probe reflectance induced by the 1 MHz modulation. The total signal measured by the lock-in is due only to signals occurring at the modulation frequency, and is dominated by the modulated probe reflectance. Phase information in the detected signal can be used in post processing of the data to subtract any nontransient noise [18]. This noise is due primarily to scattered pump light unable to be blocked from the detector, as well as the possible transmission of the AOM drive signal through electronic pathways. The dc voltage of the photodetector is also recorded for each scan and used to scale the signal measured by the lock-in. An example of the result of post processing is shown in Fig. 2. The nontransient noise evident from the initial non-zero $\Delta R/R$ signal of the raw data is removed in the phase corrected data. All scans presented in this work represent single transient reflectance scans and have been phase corrected using this procedure. While the data presented here represent individual scans, data taken at different times have been found to vary by less than 3%.

In an effort to further isolate the reflected probe light, measurements were made to detect any photoluminescence (PL) resulting from the laser excitation. This was achieved by passing all possible collected light from the sample through a monochromator and onto the photodetector. No

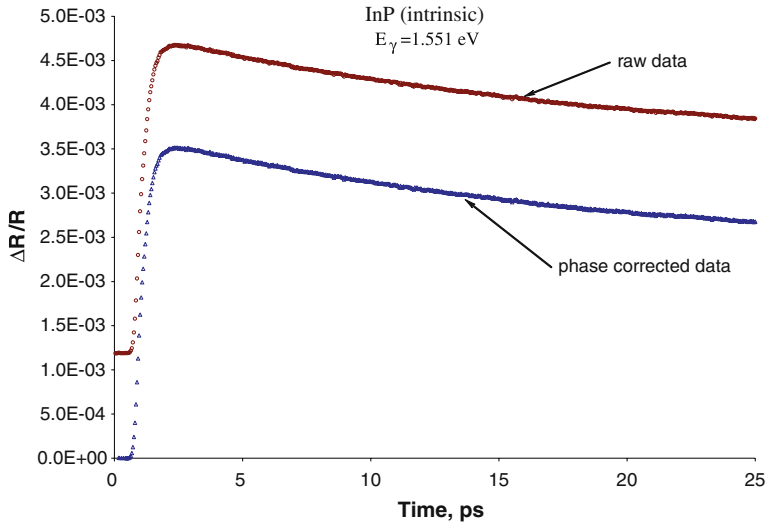

Fig. 2. The first 25 ps of raw $\Delta R/R$ data taken at a photon energy of 1.551 eV on the intrinsic InP film presented in this study. The result of the post processing phase correction is shown to remove the nontransient noise.

measurable PL signal could be detected, and it is not expected to contribute significantly to the signal seen by the detector.

5. RESULTS

The measurements presented here were performed using ultrashort laser pulses with a pulse width of $\tau_p \sim 135\,\text{fs}$, thus the *nonthermal* and *hot-excitation regimes* will be the time scales of primary interest. Since no measurable PL signal is detected, recombination during the *isothermal regime* is not observed. It is also not yet clear whether processes occurring in the *coherent regime* can be accurately detected due to the time scales of interest relative to τ_p. The goal of this investigation is to explore and identify relevant characteristics of femtosecond transient reflectance data taken on materials used for photonic devices. In particular, $\Delta R/R$ scans have shown a significant dependence on the photon energy of the excitation as well as some dependence on the pump fluence.

The experiments presented here were performed on intrinsic, Se doped n-type, and Zn doped p-type InP films. All of the films were grown by low-pressure metal-organic chemical vapor deposition (LPMOCVD) on sulfur and iron doped substrates at 630 °C [19]. The specifications for each sample and substrate are shown in Table II. For each film, scans were taken at several pump intensities over a photon energy range from 1.443 to 1.723 eV, well above the measured band gap for these films ($E_g = 1.32\,\text{eV}$). All of the $\Delta R/R$ scans cover 1500 ps of delay and exhibit many similar features. In each, the initial excitation of the probe is seen as a sharp increase in the reflectance, or $\Delta R/R$ signal. This signal then decays towards zero, but the shape of this decay varies both with photon energy, E_γ, and pump intensity. The peak of the $\Delta R/R$ signal is on the order of 10^{-3} for all of the samples at all energies. To help illustrate the features of interest in these scans, it is useful to normalize the scans.

Table II. Composition and Thickness of Each Sample

	InP	InP n-type	InP p-type
Film material	InP	InP:Se	InP:Zn
Thickness (nm)	2142	1020	1020
Doping	–	$n = 1.7 \times 10^{18}\,\text{cm}^{-3}$	$p = 1.2 \times 10^{18}\,\text{cm}^{-3}$
E_g(eV)	1.32	1.32	1.32
Substrate	InP:S	InP:Fe	InP:S

In Fig. 3, normalized $\Delta R/R$ scans of the intrinsic InP film are shown for a 200 mW pump power. The photon energy is labeled for each scan, and an inset plot of the first 6 ps is shown with the highest and lowest energy highlighted. In general, the higher energy scans exhibit a faster decay in the $\Delta R/R$ signal, but a change in curvature occurs abruptly as E_γ is increased from 1.477 to 1.591 eV. This indicates faster scattering out of the initial excitation states at higher energies. By examining the scans within the first few picoseconds, another feature is seen to develop as a function of photon energy. A dramatic change in the initial response to the pump excitation appears only at the lowest energy, 1.443 eV. In this scan, a faster initial rise followed by a decrease precedes a slower response that quickly dominates the signal.

In Fig. 4, scans of the n-type sample are plotted and exhibit many of the same features seen in the intrinsic sample. The change in the decay of the $\Delta R/R$ signal is again seen to occur between 1.513 and 1.591 eV. Also, the initial fast transient appears in the lowest energy scan, but is less pronounced than with the intrinsic sample. Scans of the p-type sample depicted in Fig. 5 once again indicate a dramatic change in the decay of the $\Delta R/R$ signal across the same spectral region, while the 1.443 eV scan has the same fast transient feature as in the other samples.

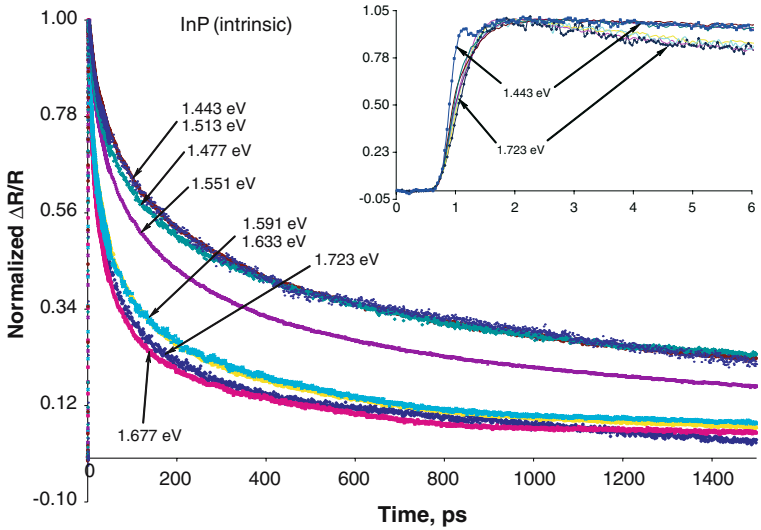

Fig. 3. Normalized $\Delta R/R$ scans for the InP (intrinsic) film with a 200 mW pump beam. Scans are labeled according to the photon energy. Inset plot shows the first 6 ps of each scan, with the highest and lowest energy scans highlighted.

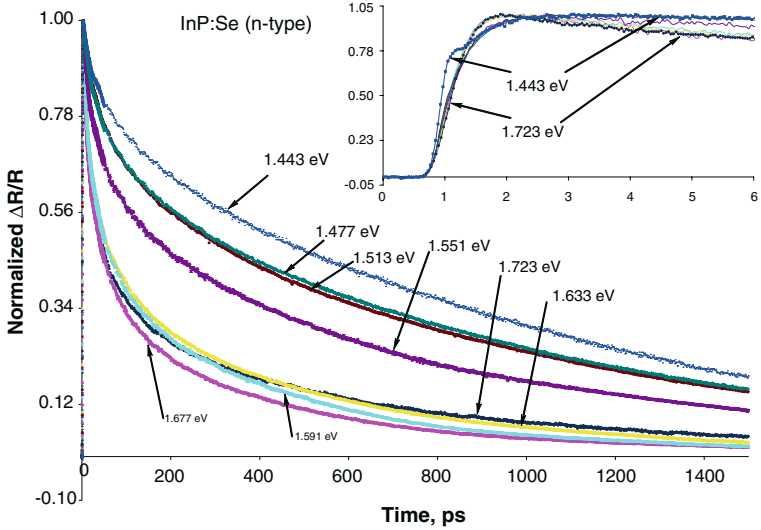

Fig. 4. Normalized $\Delta R/R$ scans for the InP:Se (n-type) film with a 200 mW pump beam.

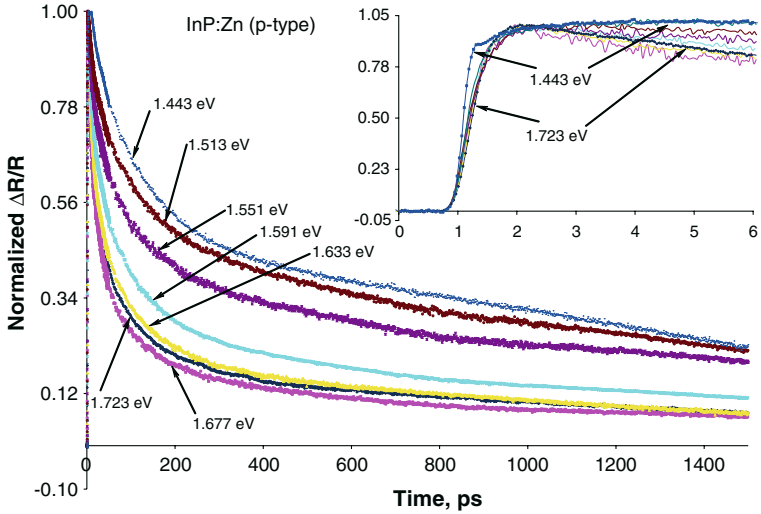

Fig. 5. Normalized $\Delta R/R$ scans for the InP:Zn (p-type) film with a 200 mW pump beam.

The energy dependent change in the decay of the $\Delta R/R$ signal seems to coincide with the energy required for transitions from the split-off band to the conduction band. The s–o band offset, Δ, has been reported to

lie ~0.11–0.20 eV below the primary valence band maximum [3,20]. This results in a transition energy of ~1.43–1.52 eV, which is close to the energy at which the decay in the scans begins to change. It is not clear at this point how these additional states affect the scattering processes involved in the relaxation of hot carriers, but they appear to contribute in a similar way for every sample. Considering the significant kink in the absorption spectrum at the s–o band energy [21], a strong change in the $\Delta R/R$ signal could be expected in this region of the spectrum.

The fast transient appearing in the 1.443 eV scans also seems to be slightly evident in the higher intensity scans at other E_γ as shown in Fig. 6 for $E_\gamma = 1.513$ eV. As previously stated, several carrier concentration dependent effects have been reported, but most studies consider a thermal distribution of carriers. As this fast transient is seen to occur on the time scale of the *coherent regime*, the carrier distribution is expected to be nonthermal. This effect on the reflectance may be evidence of bleaching, saturation of transitions in the region of E_γ, which has been observed in other ultrafast relaxation studies [22–24]. The decreased number of states participating in photon absorption at lower energies may account for the enhancement of the fast transient at lower E_γ. Bleaching could occur more readily where $D(\varepsilon)$ is smaller, but would require a higher pump fluence to completely saturate transitions where $D(\varepsilon)$ is larger. Further investigation will be necessary, particularly at the lower photon energies.

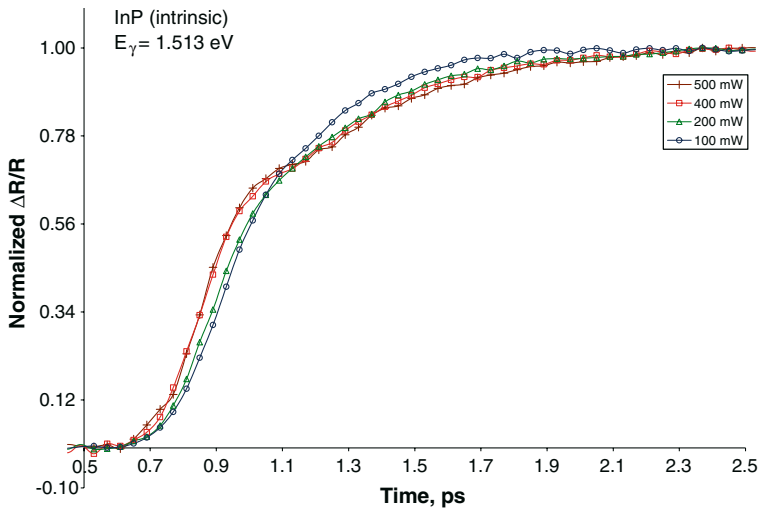

Fig. 6. Normalized $\Delta R/R$ scans for the first 2.5 ps of the InP (intrinsic) film at varying pump intensity. Evidence of the fast transient appear in the higher intensity scans.

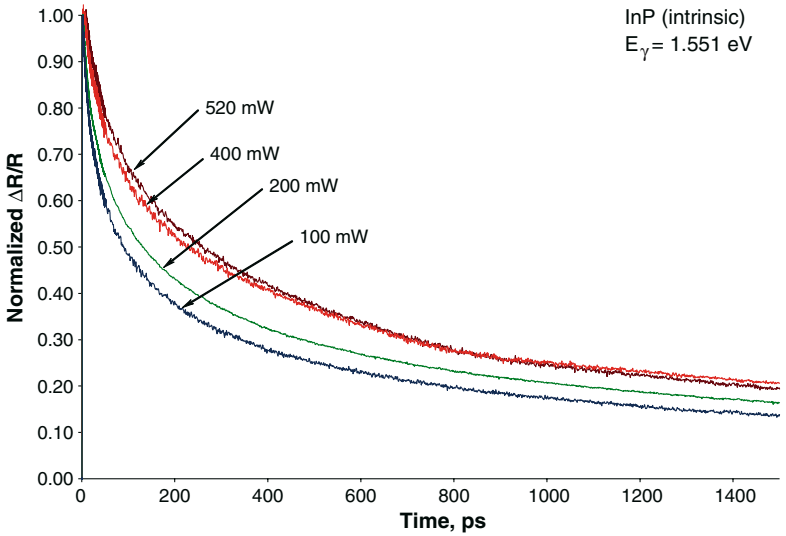

Fig. 7. Normalized $\Delta R/R$ scans for the InP (intrinsic) film at varying pump intensity.

For longer delay times, at all energies the effect of the carrier concentration on the $\Delta R/R$ response was similar for all samples. Scans were taken at 100, 200, and 400 mW at each E_γ except 1.723 eV where the power of the pump beam was limited to less than 400 mW. An additional scan was taken at each E_γ at the highest intensity possible. The results were similar for each sample over the range of E_γ, and a plot of the intrinsic sample at 1.551 eV is shown in Fig. 7. The decay of the $\Delta R/R$ response is faster at lower carrier densities (i.e., lower pump intensity). As hot carriers are scattered and fill energy states below E_γ, a reduction in e–p scattering out of states near E_γ may arise due to the reduction in available states below E_γ. At lower pump intensities, a larger number of states will remain available between E_g and E_γ and allow faster relaxation of the initial excited distribution. The results here do not provide evidence for the origin of this effect, and additional experiments must be conducted.

6. CONCLUSIONS

Experiments presented here for several InP-based films have demonstrated the sensitivity of the transient reflectance signal to both photon energy and the number of excited carriers. Experimental $\Delta R/R$ scans indicate a change in the transient behavior of the films above the energy

required for transitions originating from the spin–orbit split-off band. The origin of the carrier dependent effects and how they are related to E_γ is not yet clear but may be evidence of bleaching. Estimations of the carrier concentrations excited by the pump are on the order of $10^{18}\,\mathrm{cm}^{-3}$ using literature values for the optical constants [25]. To form a more complete understanding of the $\Delta R/R$ signal, a theoretical transient reflectance model will be developed. Part of developing a proper reflectance model will be the determination of how the optical constants are affected by the excited carrier distribution as it evolves through ultrafast dynamics. The approach being taken is to determine a functional dependence on the time-dependent excited electron distribution for the optical constants. This should allow for estimation of the rate of the thermalization, relaxation, and possibly recombination processes. It is also important to take into account any spatial gradient in the index of refraction normal to the film surface. Following the methods presented by Wait, it should be possible to include the effect of a spatially nonuniform index of refraction in the computation of the reflectance [26].

In this study, the pump and probe photon energies are equal, so the probe effectively monitors the rate at which electrons (and holes) are scattered out of the initial excited states. Future experimental studies have been proposed to enable probing states below the excited states in order to further resolve the nature of the scattering processes involved. This should also help to develop and refine an accurate transient reflectance model.

ACKNOWLEDGMENTS

Samples used for this study were generously provided by John L. Hostetler at Princeton Lightwave, Inc. The authors would also like to thank the National Science Foundation (CTS-9908372) and the Virginia Space Grant Consortium for their support of this work.

REFERENCES

1. S. W. Koch, F. Jahnke, and W. W. Chow, *Semicond. Sci. Technol*. **10**:739 (1995).
2. H. Barry Bebb and E. W. Williams, in *Transport and Optical Phenomena*, R. K. Willardson and A. C. Beer, eds. (Academic Press, New York, 1972).
3. V. Swaminathan and A. T. Macrander, *Materials Aspects of GaAs and InP Based Structures* (Prentice Hall, Englewood Cliffs, NJ, 1991).
4. Jagdeep Shah, in *Hot Carriers in Semiconductor Nanostructures — Physics and Applications*, J. Shah, ed. (Academic Press, San Diego, 1992).
5. Jagdeep Shah, *Solid-State Electron*. **21**:43 (1978).
6. W. Z. Lin, L. G. Fujimoto, and E. P. Ippen, *Appl. Phys. Lett*. **50**:124 (1987).
7. Charles Kittel, *Introduction to Solid State Physics.*, 7th Ed. (Wiley, New York, 1996).

8. J. U. Fischbach, G. Benz, N. Stath, and M. H. Pilkuhn, *Solid State Commun*. **11**:725 (1972).
9. S. C. Jain, J. M. McGregor, and D. J. Roulston, *J. Appl. Phys*. **68**:3747 (1990).
10. M. Bugajski and W. Lewandowski, *J. Appl. Phys*. **57**:521 (1985).
11. G. D. Mahen, *J. Appl. Phys*. **51**:2634 (1980).
12. E. Burstein, *Phys. Rev*. **93**:632 (1954).
13. T. S. Moss, *Proc. Phys. Soc. B* **67**:775 (1954).
14. D. von der Linde, in *Ultrashort Light Pulses, Picosecond Techniques and Applications*, S. L. Shapiro, ed. (Springer-Verlag, New York, 1977).
15. C. V. Shank and E. P. Ippen, *Appl. Phys. Lett*. **26**:62 (1975).
16. C. A. Paddock and G. L. Eesley, *J. Appl. Phys*. **60**:285 (1986).
17. H. Y. Fan, in *Optical Properties of III–V Compounds*, R. K. Willardson and A. C. Beer, eds. (Academic Press, New York, 1967).
18. Andrew N. Smith, Andrew P. Caffrey, J. Michael Klopf, and Pamela M. Norris, presented at the 35th *National Heat Transfer Conference*, Anaheim, California (2001).
19. All samples used for this study were grown and characterized at Princeton Lightwave, Inc. by John L. Hostetler, Princeton Lightwave, Inc. Cranberry, New Jersey.
20. M. L. Cohen and J. R. Chelikowsky, *Electronic Structure and Properties of Semiconductors* (Springer-Verlag, New York, 1989).
21. M. Cardona, in *Optical Properties of III–V Compounds*, R. K. Willardson and A. C. Beer, eds. (Academic Press, New York, 1967).
22. C. H. Brito Cruz, J. P. Gordon, P. C. Becker, R. L. Fork, and C. V. Shank, *IEEE J. Quantum Electron*. **24**:261 (1988).
23. E. Wintner and E. P. Ippen, *Appl. Phys. Lett*. **44**:999 (1984).
24. J. F. Reintjes, J. C. McGroddy, and A. E. Blakeslee, *J. Appl. Phys*. **46**:879 (1975).
25. S. Adachi, *Optical Constants of Crystalline and Amorphous Semiconductors Numerical Data and Graphical Information* (Kluwer Academic Publishers, Boston, 1999).
26. J. R. Wait, *Electromagnetic Waves in Stratified Media*, IEEE/OUP Series on Electromagnetic Wave Theory, D. G. Dudley, ed. (IEEE/Oxford University Press, New York, 1996).